

Article

# Enhanced Performance of Magnetic Graphene Oxide-Immobilized Laccase and Its Application for the Decolorization of Dyes

Jing Chen, Juan Leng, Xiai Yang, Liping Liao, Liangliang Liu \* and Aiping Xiao \*

Institute of Bast Fiber Crops, Chinese Academy of Agricultural Sciences, Changsha 410205, China; chenjingcaas@yahoo.com (J.C.); juanlengcaas@yahoo.com (J.L.); xiaiyang@yahoo.com (X.Y.); lipingliaocaas@yahoo.com (L.L.)

\* Correspondence: liuliangliang@caas.cn (L.L.); aipingxiao@yahoo.com (A.X.); Tel.: +86-731-88998525

Academic Editor: Rodolphe Clerac

Received: 28 December 2016; Accepted: 27 January 2017; Published: 1 February 2017

**Abstract:** In this study, magnetic graphene oxide (MGO) nanomaterials were synthesized based on covalent binding of amino  $\text{Fe}_3\text{O}_4$  nanoparticles onto the graphene oxide (GO), and the prepared MGO was successfully applied as support for the immobilization of laccase. The MGO-laccase was characterized by transmission electron microscopy (TEM) and a vibrating sample magnetometer (VSM). Compared with free laccase, the MGO-laccase exhibited better pH and thermal stabilities. The optimum pH and temperature were confirmed as pH 3.0 and 35 °C. Moreover, the MGO-laccase exhibited sufficient magnetic response and satisfied reusability after being retained by magnetic separation. The MGO-laccase maintained 59.8% activity after ten uses. MGO-laccase were finally utilized in the decolorization of dye solutions and the decolorization rate of crystal violet (CV), malachite green (MG), and brilliant green (BG) reached 94.7% of CV, 95.6% of MG, and 91.4% of BG respectively. The experimental results indicated the MGO-laccase nanomaterials had a good catalysis ability to decolorize dyes in aqueous solution. Compared with the free enzyme, the employment of MGO as enzyme immobilization support could efficiently enhance the availability and facilitate the application of laccase.

**Keywords:** dyes; graphene oxide; laccase; magnetic nanoparticles

## 1. Introduction

Enzymes are biological catalysts with excellent catalysis properties in various fields [1]. Because of the high activity and specificity, enzymes are widely used in industrial biosynthesis and environmental protection [2]. However, enzymes are expensive, unstable in complicated solution environments, and difficult to separate from solution. Enzyme immobilization could effectively prolong the activity, improve the stability, and provide the reusability of enzyme [3,4]. Immobilized enzymes also showed higher pH and temperature endurance range, satisfied stability, and simple product purification [5,6].

Various inorganic and organic nanomaterials such as silica nanoparticles, carbon nanotubes, gold nanoparticles, and metal oxide nanoparticles have been used as carriers to immobilize enzymes [7–11]. Among them, magnetic nanomaterials show many advantages including large surface areas for high immobilization amount of enzymes, facile modification, simple separation with a magnet, and high reusability [12]. Graphene oxide (GO) has also attracted the attention of researchers due to its typical large surface area, good biocompatibility, excellent stability, and high adsorption capacity. GO contains carboxyl, hydroxyl, and epoxy groups and was generally applied in drug delivery, sensors, and nanocomposites [13]. The combination of magnetic nanomaterials and GO remain an advantage of these two materials. The magnetic response property, large surface area, two-dimensional structure,

easy surface modification, large enzyme immobilization capacity, simple preparation, and satisfactory reusability of magnetic GO (MGO) has received considerable attention in enzyme immobilization and related research [14,15]. MGO and graphene-based magnetic nanocomposites were synthesized as enzyme immobilization support for catalase, glucoamylase, lipase, and  $\beta$ -galactosidase [15–19]. The synthesized immobilized enzyme showed high activity recovery, easy recycling, improved catalytic activity, and stability compared to the free enzyme. However, the immobilization of laccase on MGO has seldom been reported.

Water pollution has been a universal crisis in modern industry over the years. Especially, dye wastewater is one of the most serious problems because of the many kinds of dyes used in the textile, paper, and food industries. Most dyes and pigments are toxic, complex, have low biodegradability, and are carcinogenic. They have been shown to cause much damage due to the resistance to degradation and the perilous affect to plants, aquatic organisms, and human beings [20]. Triphenylmethane dyes consisting of crystal violet (CV) and malachite green (MG) and azo dyes such as brilliant green (BG) were all widely used in various industries. Dye wastewater can be treated by conventional physical and chemical methods including adsorption, coagulation, and oxidation [21–23]. Among them, dye decolorization using enzymes such as laccase has gained great attention due to its processing efficiency [24,25].

Laccase (EC 1.10.3.2) is a copper-containing oxidase widely distributed in plants, insects, and fungi [26]. Laccase mainly catalyze the polymerization or depolymerization processes of lignin formation in plants. It is widely used in the textile, dyeing, and printing industries for the decolorization of dyes and pulp and the delignification of woody biomass [27]. In addition, laccase can be applied to the oxidation of various phenolic and non-phenolic compounds including various dyestuffs and environmental pollutants [28]. Based on previous reports, laccase has received attention for the treatment of dyes and phenolic compounds. Dye decolorization using immobilized laccase has also been reported in recent years [24,29]. Therefore, using laccase and immobilized laccase as a biocatalyst for the decolorization of dyes is a promising prospect.

Enzyme immobilization methods include entrapment, cross-linking, physical adsorption, and covalent binding to supports. Among these, covalent binding has shown advantages in forming stable binding between enzymes and supports [30]. Bifunctional cross-linking agents such as glutaraldehyde, maleic anhydride, and genipin are important in the immobilization of enzymes [31]. In this study, MGO-immobilized laccase (MGO-laccase) was synthesized and applied in the decolorization of CV, MG, and BG. Laccase and amino  $\text{Fe}_3\text{O}_4$  nanoparticles were covalently bound on GO after the activation of GO using 1-ethyl-3-(3-dimethylaminopropyl) carbodiimide (EDC) and N-hydroxy sulfosuccinimide (NHS) as the bifunctional cross-linking agents. The prepared MGO and MGO-laccase were characterized by transmission electron microscopy (TEM) and a vibration sample magnetometer (VSM). In order to obtain the optimum reaction condition, the activities of free laccase and MGO-laccase at different pH and temperature conditions were measured and compared. At the optimum condition, highly efficient decolorization of CV, MG, and BG was achieved by MGO-laccase.

## 2. Results and Discussion

### 2.1. Characterizations of MGO-Laccase

Figure 1 shows the TEM characterization images of amino  $\text{Fe}_3\text{O}_4$  nanoparticles and MGO-laccase. The amino  $\text{Fe}_3\text{O}_4$  nanoparticles presented a round shape, and the average diameter is about 200 nm in Figure 1a. The shape and size of amino  $\text{Fe}_3\text{O}_4$  nanoparticles are in accord with other reported values [32]. After the combination of GO, it can be clearly seen in Figure 1b that amino  $\text{Fe}_3\text{O}_4$  nanoparticles steadily bound with GO. The sheet structure with a wrinkled edge of GO has been seen previously [33].

The magnetic properties of amino  $\text{Fe}_3\text{O}_4$  nanoparticles, MGO, and MGO-laccase were investigated using a VSM at room temperature, and their magnetization curves are shown in Figure 2.

The maximum saturation magnetizations of MGO-laccase were 24.0 emu/g, which was lower than that of amino  $\text{Fe}_3\text{O}_4$  nanoparticles (74.9 emu/g) and MGO (31.5 emu/g). The lower maximum saturation magnetizations of MGO-laccase was due to the increasing amount of nonmagnetic GO and laccase on the surface after functionalization and the relatively reduced amount of  $\text{Fe}_3\text{O}_4$  nanoparticles [34,35]. Although the maximum saturation magnetizations of MGO-laccase declined to a certain extent, it still had an accepted magnetic response for rapid separation from the reaction medium [36].

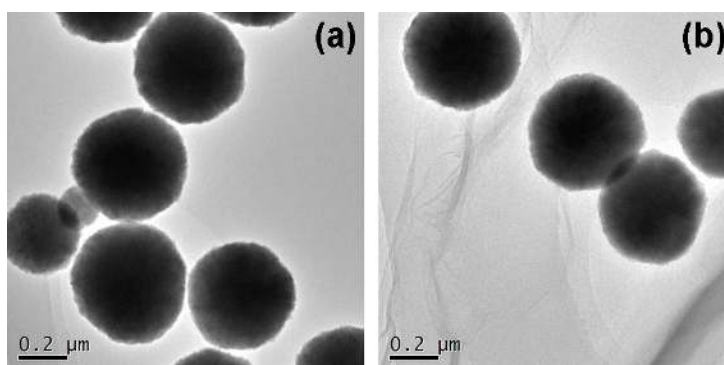


**Figure 1.** The TEM images of (a) amino  $\text{Fe}_3\text{O}_4$  nanoparticles and (b) MGO-laccase.

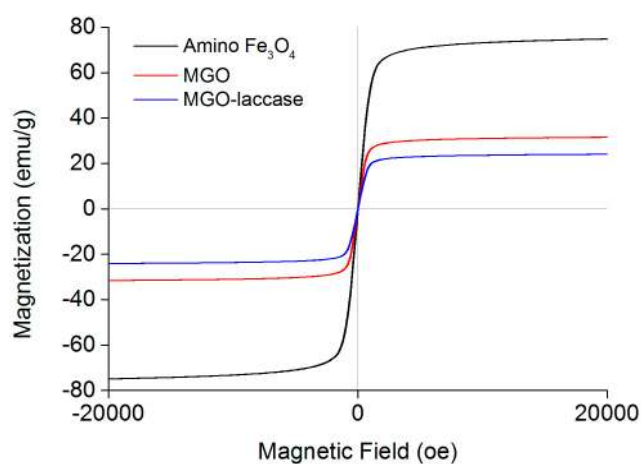


**Figure 2.** The magnetization curves of amino  $\text{Fe}_3\text{O}_4$  nanoparticles (black), MGO (red), and MGO-laccase (blue).

## 2.2. Immobilization of Laccase on MGO-Laccase

The concentration of laccase affected the immobilization, and it needed to be optimized to obtain the maximum amount of retained activity and enzyme immobilization. Therefore, the immobilization amounts of laccase on MGO, the retained activities of MGO-laccase, and the relative activities after immobilization were all investigated. As shown in Figure 3, the immobilization amount of laccase and the relative activity of MGO-laccase increased with the increase in laccase concentration and reached the highest (the immobilization amount of laccase was 30.0 mg/g and the relative activity of MGO-laccase was 97.9%) when the concentration of laccase was 5.0 mg/mL. Meanwhile, the retained activities of MGO-laccase reached 96% and 97.9% when the concentration of laccase was 4.0 and 5.0 mg/mL, respectively. However, a reduction of data was observed when the concentration of laccase was more than 5.0 mg/mL. This might be because excessive enzymes blocked the intermolecular space and restrained the transmission of substrate [37]. As a result, the optimum concentration of laccase was set at 5.0 mg/mL.

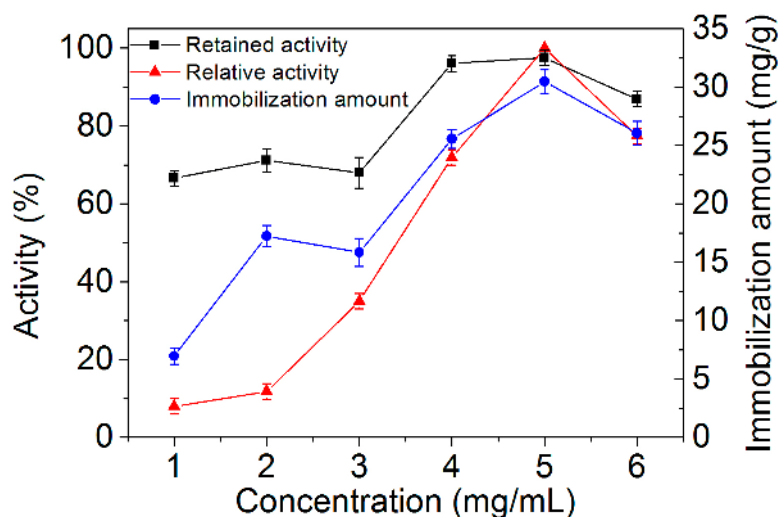


**Figure 3.** Immobilization amounts of laccase, retained activities of immobilized laccase on MGO-laccase, and relative activities of MGO-laccase at different laccase concentrations (1.0–6.0 mg/mL).

### 2.3. Effect of pH on the Activities of Free Laccase and MGO-Laccase

The effect of pH on the activities of free laccase and MGO-laccase were investigated at room temperature in the pH range 2.0–8.0, and the results are shown in Figure 4. The highest activity of the free laccase and MGO-laccase was individually considered as 100% and the activities at the other pH were noted proportional to the corresponding highest values. As shown in Figure 4, free laccase and MGO-laccase exhibited the maximum activity at pH 3.0. When pH was higher than 3.0, the activity of free laccase decreased sharply, while MGO-laccase showed relatively higher activity compared to that of free laccase. As reported, the stability of fungal laccases is generally higher at acidic pH. Diao and coauthors mentioned that the optimal pH for the activity of immobilized *Panus conchatus* laccase is 3.2 [38]. The improved pH tolerance of MGO-laccase against pH changes in solution is attributed to the buffer function of GO. In an acidic medium, the hydrogen ions are attracted and consumed by the negatively charged GO, which is helpful in preventing the hydrogen ions from contacting with the enzymes [39,40]. The improved performance might also be due to the conformational changes resulting in a suitable open conformation, with few restrictions to substrates produced by immobilization. These result is in agreement with other studies [41].

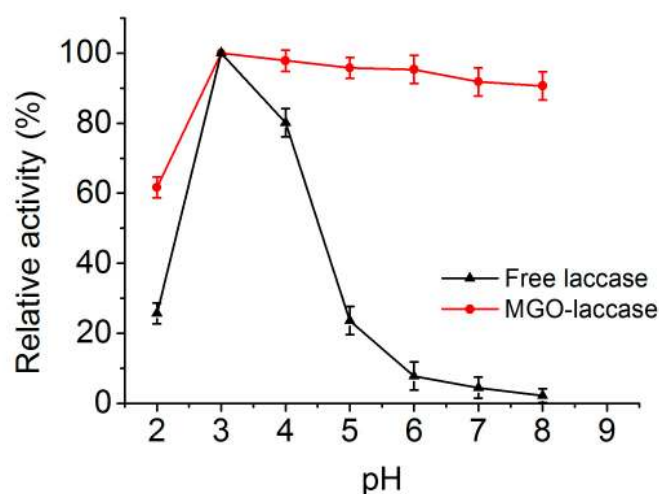


**Figure 4.** Effect of pH on the activities of free laccase (black) and MGO-laccase (red).

#### 2.4. Effect of Temperature on the Activities of Free Laccase and MGO-Laccase

The effect of temperature on the activities of free laccase and MGO-laccase was assayed at pH 3.0 and different temperatures in a range of 5–65 °C. The highest activity of the free laccase and MGO-laccase was individually considered as 100%, and the activities at the other temperatures were noted to be proportional to the corresponding highest values. As seen in Figure 5, the highest activities of free laccase and MGO-laccase both occurred at 35 °C. When the temperature increased from 35 to 65 °C, the activities of free laccase and MGO-laccase decreased because of the enzyme deactivation at relative high temperatures. However, MGO-laccase showed relatively higher activity compared with that of free laccase at high temperature, which means less sensitivity to temperature and more rigidity in conformational changes. This result was probably due to the strength of interactions between enzyme and matrix or a low restriction in the substrate diffusion [42].

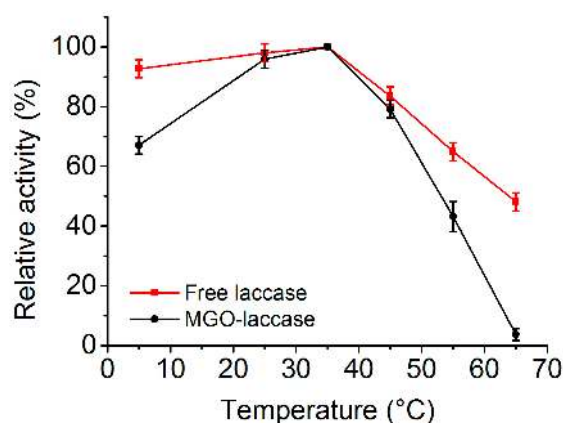


Figure 5. Effect of temperature on the activities of free laccase (black) and MGO-laccase (red).

#### 2.5. Reusability of MGO-Laccase

The reusability of immobilized enzyme was an important factor for practical applications to make the process economic and feasible. The activity of MGO-laccase remained 59.8% even after ten consecutive cycles of reuse (Figure 6). This result indicates that the MGO-laccase exhibits appropriate reusability in consecutive cycles of reuse. The reduction in residual activity over the ten cycles might be because of the aggregation of nanomaterials, the enzyme leakage from the supporters, and the deactivation of enzyme [9,43]. Considering the simple and rapid separation from reaction solution by an ordinary magnet, the MGO-laccase could be reused repeatedly in order to reduce the cost and simplify the processes.

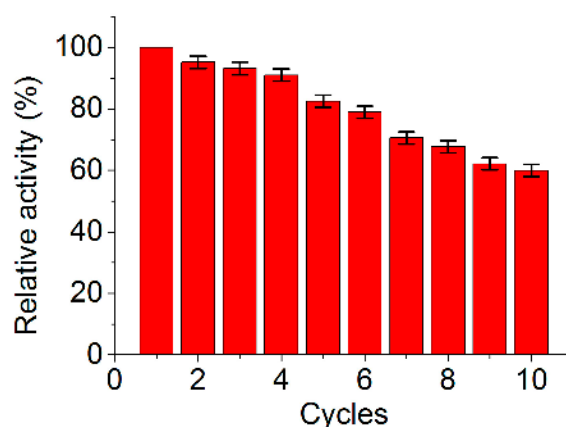


Figure 6. Reusability of MGO-laccase over ten consecutive cycles.

## 2.6. Decolorization of Dyes

The decolorization capacities of various dyes including CV, MG, and BG using free laccase and MGO-laccase were both assessed. As shown in Figure 7, 93.0% of CV, 88.2% of MG, and 90.8% of BG was respectively decolorized after 180 min incubation with free laccase in the optimum conditions. Meanwhile, 94.7% of CV, 95.6% of MG, and 91.4% of BG was respectively decolorized with MGO-laccase after 180 min of incubation. However, as a comparison, the decolorization ability of MGO was tested, and the result showed that only 13.2% of dyes decolorized after 180 min of incubation was reached. In general, the decolorization capacities of free laccase were equal to or even lower than that of the immobilized laccase. Obviously, MGO-laccase exhibited good decolorization capacity to dye solutions in this work. Combined with the appropriate reusability in consecutive cycles of reuse, the MGO-laccase is suitable as material efficient in the decolorization of dyes from aqueous solutions.

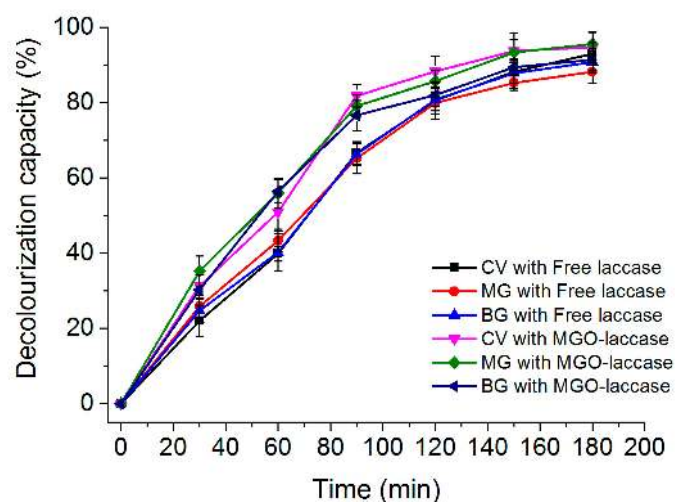


Figure 7. The removal rates of dyes (CV, MG, and BG) with free laccase and MGO-laccase.

## 3. Materials and Methods

### 3.1. Materials

Laccase from *Trametes versicolor*, 2,2-azinobis-3-ethylbenzothiazoline-6-sulfonate (ABTS), 1-ethyl-3-(3-dimethylaminopropyl) carbodiimide (EDC), *N*-hydroxy sulfosuccinimide (NHS), 3-aminopropyltriethoxysilane, and glutaraldehyde were acquired from Sigma-Aldrich Chemicals (St. Louis, MO, USA). Crystal violet (CV), malachite green (MG), and brilliant green (BG) were obtained commercially from Aladdin (Shanghai, China). Graphite flake (100 mesh) was purchased from Nanjing XFNANO Materials Tech Co., Ltd. (Nanjing, China). Ultrapure water (18.2 M $\Omega$  cm resistivity) was obtained from an ELGA water purification system (ELGA Berkefeld, Veolia, Germany). All other chemicals were analytical grade and purchased from Sinopharm Chemical Reagent Co., Ltd. (Shanghai, China).

### 3.2. Preparation of Amino Fe<sub>3</sub>O<sub>4</sub> Nanoparticles

An amount of 1.300 g of ferric chloride, 1.000 g of PEG 6000 and 3.600 g of anhydrous sodium acetate were poured in 40 mL of ethyleneglycol under stirring and ultrasonication. The mixture was then transferred into an autoclave and maintained at 180 °C for 6 h. After reaction, the products were collected by a magnet and washed with ethanol solution three times. Finally, Fe<sub>3</sub>O<sub>4</sub> nanoparticles were dried in vacuum at 60 °C for further use.

One hundred milligrams of Fe<sub>3</sub>O<sub>4</sub> nanoparticles were dispersed in 200 mL of 99% ethanol solution under mechanical agitation. Then, 2 mL of 3-aminopropyltriethoxysilane was added dropwise, and the

solution was stirred with mechanical agitation at 25 °C for 6 h. The final amino Fe<sub>3</sub>O<sub>4</sub> nanoparticles were washed with ethanol three times and dried in vacuum at 60 °C.

### 3.3. Preparation of GO

One gram of graphite flakes and 6.000 g KMnO<sub>4</sub> were slowly added into the mixture containing 120 mL of concentrated sulfuric acid and 13 mL of phosphoric acid. After being maintained at 50 °C for 12 h under magnetic agitation, the mixed solution was poured into 130 mL of ice containing H<sub>2</sub>O<sub>2</sub>. Then, the products were centrifuged at 10,000 rpm for 10 min. The supernatant was decanted, and the solid was washed with 30% hydrochloric acid and water five times, respectively.

### 3.4. Preparation of MGO-Laccase

In order to activate the carboxyl group of GO, 10 mL of EDC/NHS mixture (5 mg/mL of EDC and 3 mg/mL of NHS) was added to 10 mL of GO solution (1 mg/mL in water) and shaken at 25 °C for 30 min. Then, 10 mg of amino Fe<sub>3</sub>O<sub>4</sub> nanoparticles and 2 mL of laccase were added into the activated GO solution. The mixture was then shaken at 25 °C for 1 h. After reaction, the excess enzyme solution was decanted by magnetic separation. The MGO-laccase were washed with phosphate buffer solution three times and dispersed in PBS for further use.

### 3.5. Characterizations and Measurements

Transmission electron micrographs (TEM) were obtained on a JEM-2100 electron microscope (JEOL, Akishima, Japan). A small amount of sample powder was dispersed in ethanol and dropped on a holey carbon coated copper grid before TEM characterization. Magnetization curves were recorded on a vibration sample magnetometer VSM7307 (Lake Shore, Westerville, Ohio, USA) at room temperature. UV-Vis spectra were recorded on UV-2600 UV-VIS Spectrophotometer (Shimadzu, Kyoto, Japan). In order to investigate the immobilization capacity of the materials, the immobilization amounts of laccase on MGO were performed and calculated by subtracting the amount of enzyme in the supernatant from the amount of total enzyme used for immobilization by Bradford's method [44]. The retained activity of MGO-laccase is calculated according to Equation (1):

$$\text{Retained activity} = V_i/V_f \times 100\% \quad (1)$$

where  $V_i$  is the activity of MGO-laccase and  $V_f$  is the activity of the same amount of free laccase as that immobilized on MGO-laccase [45]. The relative activity of MGO-laccase is expressed as relative forms (%) with the maximal value of activity at a certain concentration set as 100% [46]. Three replications of all assays were conducted in this study.

### 3.6. Laccase Activity Assay

The activities of free laccase and MGO-laccase were determined by a UV-Vis spectrophotometer using ABTS as the substrate. Briefly, 1.0 mL of laccase (5.0 mg/mL, pH 3.0) or MGO-laccase (10 mg) and 0.5 mol/mL of ABTS (2.0 mL, pH 3.0) were mixed and incubated at 30 °C for 20 min. The absorbance of the solutions was measured at 420 nm. The same amount of water instead of enzyme solution was used as a blank test. One laccase activity unit (U) is defined as the amount of enzyme required to oxidize 1 μmol of ABTS per minute. Three replications of all assays were conducted.

To determine the effect of pH on the activity of the enzyme, free laccase and MGO-laccase were respectively incubated in citrate-phosphate buffers, with pH ranging from 2.0 to 8.0 at 25 °C for 15 min, and the activities were then assayed. Meanwhile, the effect of temperature on enzyme activity was determined by incubating free laccase and MGO-laccase in citrate-phosphate buffers (0.1 M, pH 3.0) for 15 min at different temperatures ranging from 5 to 65 °C before activity assays.

### 3.7. Reusability of MGO-Laccase

The reusability of MGO-laccase was evaluated by performing several consecutive operating cycles using ABTS solution as the substrate. After a previous test, the mixture was separated with magnet and the solution was determined by the UV-Vis spectrophotometer. The MGO-laccase was reused by washing excessively with water. Then, the MGO-laccase was transferred into a fresh ABTS solution to start a new cycle. The activity of MGO-laccase in each cycle was measured and shown as relative value. The activity of the first cycle was set as 100%.

### 3.8. Decolorization of Dyes with Free Laccase and MGO-Laccase

The decolorization capacities of various dyes with free laccase and MGO-laccase were conducted, and the decrease in absorbance at the maximum absorption wavelength of each dye (584 nm for CV, 618 nm for MG, and 625 nm for BG) was monitored by a UV-Vis spectrophotometer. One milliliter of laccase (5.0 mg/mL, pH 3.0) or MGO-laccase (10 mg) was mixed with 3.0 mL of dye solution (CV, MG, and BG, 50.0 mg/L) in a citrate-phosphate buffer (0.1 M, pH 3.0). The mixtures were incubated at 35 °C with a shaking speed of 250 rpm in darkness. The blank control used water instead of a free enzyme solution. Experiments were all performed in triplicate. Decolorization capacity was expressed in terms of percentage and calculated as Equation (2):

$$\text{Decolorization capacity} = (A_i - A_0) / A_i \times 100\% \quad (2)$$

where  $A_i$  is the initial absorbance of the dye solution, and  $A_0$  is the final absorbance of dye after treatment at a certain time.

## 4. Conclusions

In summary, the immobilization of laccase on MGO nanomaterials was successfully achieved. Compared to the free laccase, MGO-laccase showed improved thermal and pH stabilities. At the optimum pH and temperature conditions (pH 3.0 and 35 °C), the MGO-laccase exhibited sufficient magnetic response and satisfactory reusability. The MGO-laccase recovered 59.8% activity after ten uses. MGO-laccase was then utilized in the decolorization of dye solutions and the removal of crystal violet (CV), malachite green (MG), and brilliant green (BG) reached 94.7%, 95.6%, and 91.4% in aqueous solution. The experimental results indicated that the MGO-laccase nanomaterials effectively improved the processing efficiency and expanded the industrial application of enzymes.

**Acknowledgments:** This work was supported by the risk assessment of agricultural products quality and safety project (GJFP2017010).

**Author Contributions:** Jing Chen, Liping Liao, and Liangliang Liu performed the experiments and analyzed the data; Liangliang Liu and Aiping Xiao conceived and designed the experiments; Xia Yang and Juan Leng wrote the paper; Aiping Xiao and Liangliang Liu revised the paper.

**Conflicts of Interest:** The authors declare no conflict of interest.

## References

1. Jain, P.; Das, S.; Chakma, B.; Goswami, P. Aptamer-graphene oxide for highly sensitive dual electrochemical detection of Plasmodium lactate dehydrogenase. *Anal. Biochem.* **2016**, *514*, 32–37. [[CrossRef](#)] [[PubMed](#)]
2. Long, Q.; Fang, A.J.; Wen, Y.Q.; Li, H.T.; Zhang, Y.Y.; Yao, S.Z. Rapid and highly-sensitive uric acid sensing based on enzymatic catalysis-induced upconversion inner filter effect. *Biosens. Bioelectron.* **2016**, *86*, 109–114. [[CrossRef](#)] [[PubMed](#)]
3. Homaei, A. Immobilization of *Penaeus merguensis* alkaline phosphatase on gold nanorods for heavy metal detection. *Ecotox. Environ. Saf.* **2017**, *136*, 1–7. [[CrossRef](#)] [[PubMed](#)]
4. Tan, C.Y.; Hirakawa, H.; Suzuki, R.; Haga, T.; Iwata, F.; Nagamune, T. Immobilization of a Bacterial Cytochrome P450 Monooxygenase System on a Solid Support. *Angew. Chem. Int. Edit.* **2016**, *55*, 15002–15006. [[CrossRef](#)] [[PubMed](#)]



5. Bilal, M.; Asgher, M.; Iqbal, H.M.N.; Hu, H.B.; Zhang, X.H. Gelatin-Immobilized Manganese Peroxidase with Novel Catalytic Characteristics and Its Industrial Exploitation for Fruit Juice Clarification Purposes. *Catal. Lett.* **2016**, *146*, 2221–2228. [[CrossRef](#)]
6. Bavaro, T.; Cattaneo, G.; Serra, I.; Benucci, I.; Pregnotato, M.; Terreni, M. Immobilization of Neutral Protease from *Bacillus subtilis* for Regioselective Hydrolysis of Acetylated Nucleosides: Application to Capecitabine Synthesis. *Molecules* **2016**, *21*, 1621. [[CrossRef](#)] [[PubMed](#)]
7. Escuin, P.C.; Garcia-Bennett, A.; Ros-Lis, J.V.; Foix, A.A.; Andres, A. Application of mesoporous silica materials for the immobilization of polyphenol oxidase. *Food Chem.* **2017**, *217*, 360–363. [[CrossRef](#)] [[PubMed](#)]
8. Hajar, M.; Vahabzadeh, F. Biolubricant production from castor oil in a magnetically stabilized fluidized bed reactor using lipase immobilized on Fe<sub>3</sub>O<sub>4</sub> nanoparticles. *Ind. Crop. Prod.* **2016**, *94*, 544–556. [[CrossRef](#)]
9. Liu, N.; Liang, G.; Dong, X.W.; Qi, X.L.; Kim, J.; Piao, Y. Stabilized magnetic enzyme aggregates on graphene oxide for high performance phenol and bisphenol A removal. *Chem. Eng. J.* **2016**, *306*, 1026–1034. [[CrossRef](#)]
10. Ulu, A.; Koytepe, S.; Ates, B. Design of starch functionalized biodegradable P(MAA-co-MMA) as carrier matrix for L-asparaginase immobilization. *Carbohydr. Polym.* **2016**, *153*, 559–572. [[CrossRef](#)] [[PubMed](#)]
11. Shrestha, B.K.; Ahmad, R.; Mousa, H.M.; Kim, I.G.; Kim, J.I.; Neupane, M.P.; Park, C.H.; Kim, C.S. High-performance glucose biosensor based on chitosan-glucose oxidase immobilized polypyrrole/Nafion/functionalized multi-walled carbon nanotubes bio-nanohybrid film. *J. Colloid Interf. Sci.* **2016**, *482*, 39–47. [[CrossRef](#)] [[PubMed](#)]
12. Gawande, M.B.; Branco, P.S.; Varma, R.S. Nano-magnetite (Fe<sub>3</sub>O<sub>4</sub>) as a support for recyclable catalysts in the development of sustainable methodologies. *Chem. Soc. Rev.* **2013**, *42*, 3371–3393. [[CrossRef](#)] [[PubMed](#)]
13. Georgakilas, V.; Tiwari, J.N.; Kemp, K.C.; Perrnan, J.A.; Bourlinos, A.B.; Kim, K.S.; Zboril, R. Noncovalent Functionalization of Graphene and Graphene Oxide for Energy Materials, Biosensing, Catalytic, and Biomedical Applications. *Chem. Rev.* **2016**, *116*, 5464–5519. [[CrossRef](#)] [[PubMed](#)]
14. Wu, L.X.; Yu, L.; Ding, X.X.; Li, P.W.; Dai, X.H.; Chen, X.M.; Zhou, H.Y.; Bai, Y.Z.; Ding, J. Magnetic solid-phase extraction based on graphene oxide for the determination of lignans in sesame oil. *Food Chem.* **2017**, *217*, 320–325. [[CrossRef](#)] [[PubMed](#)]
15. Chang, Q.; Huang, J.; Ding, Y.; Tang, H. Catalytic Oxidation of Phenol and 2,4-Dichlorophenol by Using Horseradish Peroxidase Immobilized on Graphene Oxide/Fe<sub>3</sub>O<sub>4</sub>. *Molecules* **2016**, *21*, 1044. [[CrossRef](#)] [[PubMed](#)]
16. Khan, M.; Husain, Q.; Naqvi, A.H. Graphene based magnetic nanocomposites as versatile carriers for high yield immobilization and stabilization of [small beta]-galactosidase. *RSC Adv.* **2016**, *6*, 53493–53503. [[CrossRef](#)]
17. Amirbandeh, M.; Taheri-Kafrani, A. Immobilization of glucoamylase on triazine-functionalized Fe<sub>3</sub>O<sub>4</sub>/graphene oxide nanocomposite: Improved stability and reusability. *Int. J. Biol. Macromol.* **2016**, *93*, 1183–1191. [[CrossRef](#)] [[PubMed](#)]
18. Yang, D.; Wang, X.; Shi, J.; Wang, X.; Zhang, S.; Han, P.; Jiang, Z. In situ synthesized rGO-Fe<sub>3</sub>O<sub>4</sub> nanocomposites as enzyme immobilization support for achieving high activity recovery and easy recycling. *Biochem. Eng. J.* **2016**, *105*, 273–280. [[CrossRef](#)]
19. Hou, C.; Zhou, L.; Zhu, H.; Wang, X.; Hu, N.; Zeng, F.; Wang, L.; Yin, H. Mussel-inspired surface modification of magnetic@graphite nanosheets composite for efficient *Candida rugosa* lipase immobilization. *J. Ind. Microbiol. Biot.* **2015**, *42*, 723–734. [[CrossRef](#)] [[PubMed](#)]
20. Atta, A.; Al-Lohedan, H.; Tawfik, A.; Ezzat, A. Application of Super-Amphiphilic Silica-Nanogel Composites for Fast Removal of Water Pollutants. *Molecules* **2016**, *21*, 1392. [[CrossRef](#)] [[PubMed](#)]
21. Yang, C.H.; Shih, M.C.; Chiu, H.C.; Huang, K.S. Magnetic Pycnopus sanguineus-Loaded Alginate Composite Beads for Removing Dye from Aqueous Solutions. *Molecules* **2014**, *19*, 8276–8288. [[CrossRef](#)] [[PubMed](#)]
22. Saber-Samandari, S.; Saber-Samandari, S.; Joneidi-Yekta, H.; Mohseni, M. Adsorption of anionic and cationic dyes from aqueous solution using gelatin-based magnetic nanocomposite beads comprising carboxylic acid functionalized carbon nanotube. *Chem. Eng. J.* **2017**, *308*, 1133–1144. [[CrossRef](#)]
23. Navarro, P.; Gabaldon, J.A.; Gomez-Lopez, V.M. Degradation of an azo dye by a fast and innovative pulsed light/H<sub>2</sub>O<sub>2</sub> advanced oxidation process. *Dyes Pigm.* **2017**, *136*, 887–892. [[CrossRef](#)]
24. Nguyen, T.A.; Fu, C.C.; Juang, R.S. Effective removal of sulfur dyes from water by biosorption and subsequent immobilized laccase degradation on crosslinked chitosan beads. *Chem. Eng. J.* **2016**, *304*, 313–324. [[CrossRef](#)]

25. Nguyen, L.N.; Hai, F.I.; Dosseto, A.; Richardson, C.; Price, W.E.; Nghiem, L.D. Continuous adsorption and biotransformation of micropollutants by granular activated carbon-bound laccase in a packed-bed enzyme reactor. *Bioresource Technol.* **2016**, *210*, 108–116. [[CrossRef](#)] [[PubMed](#)]
26. Yang, J.; Lin, Y.H.; Yang, X.D.; Ng, T.B.; Ye, X.Y.; Lin, J. Degradation of tetracycline by immobilized laccase and the proposed transformation pathway. *J. Hazard. Mater.* **2017**, *322*, 525–531. [[CrossRef](#)] [[PubMed](#)]
27. Du, P.; Zhao, H.; Liu, C.; Huang, Q.; Cao, H. Transformation and products of captopril with humic constituents during laccase-catalyzed oxidation: role of reactive intermediates. *Water Res.* **2016**, *106*, 488–495. [[CrossRef](#)] [[PubMed](#)]
28. Saravanakumar, T.; Park, H.S.; Mo, A.Y.; Choi, M.S.; Kim, D.H.; Park, S.M. Detoxification of furanic and phenolic lignocellulose derived inhibitors of yeast using laccase immobilized on bacterial cellulosic nanofibers. *J. Mol. Catal. B-Enzym.* **2016**, *134*, 196–205. [[CrossRef](#)]
29. Dai, Y.R.; Yao, J.; Song, Y.H.; Liu, X.L.; Wang, S.Y.; Yuan, Y. Enhanced performance of immobilized laccase in electrospun fibrous membranes by carbon nanotubes modification and its application for bisphenol A removal from water. *J. Hazard. Mater.* **2016**, *317*, 485–493. [[CrossRef](#)] [[PubMed](#)]
30. Jian, H.; Wang, Y.; Bai, Y.; Li, R.; Gao, R. Site-Specific, Covalent Immobilization of Dehalogenase ST2570 Catalyzed by Formylglycine-Generating Enzymes and Its Application in Batch and Semi-Continuous Flow Reactors. *Molecules* **2016**, *21*, 895. [[CrossRef](#)] [[PubMed](#)]
31. Kahar, U.; Sani, M.; Chan, K.G.; Goh, K. Immobilization of  $\alpha$ -Amylase from *Anoxybacillus* sp. SK3-4 on ReliZyme and Immobead Supports. *Molecules* **2016**, *21*, 1196. [[CrossRef](#)] [[PubMed](#)]
32. Li, Y.; Xu, X.; Deng, C.; Yang, P.; Zhang, X. Immobilization of Trypsin on Superparamagnetic Nanoparticles for Rapid and Effective Proteolysis. *J. Proteome Res.* **2007**, *6*, 3849–3855. [[CrossRef](#)] [[PubMed](#)]
33. Liu, J.; Wang, H.; Li, X.; Jia, W.; Zhao, Y.; Ren, S. Recyclable magnetic graphene oxide for rapid and efficient demulsification of crude oil-in-water emulsion. *Fuel* **2017**, *189*, 79–87. [[CrossRef](#)]
34. Waifalkar, P.P.; Parit, S.B.; Chougale, A.D.; Sahoo, S.C.; Patil, P.S.; Patil, P.B. Immobilization of invertase on chitosan coated  $\gamma$ -Fe<sub>2</sub>O<sub>3</sub> magnetic nanoparticles to facilitate magnetic separation. *J. Colloid Interf. Sci.* **2016**, *482*, 159–164. [[CrossRef](#)] [[PubMed](#)]
35. Wang, J.; Zhao, G.; Li, Y.; Zhu, H.; Peng, X.; Gao, X. One-step fabrication of functionalized magnetic adsorbents with large surface area and their adsorption for dye and heavy metal ions. *Dalton Trans.* **2014**, *43*, 11637–11645. [[CrossRef](#)] [[PubMed](#)]
36. Vu, H.C.; Dwivedi, A.D.; Le, T.T.; Seo, S.H.; Kim, E.J.; Chang, Y.S. Magnetite graphene oxide encapsulated in alginate beads for enhanced adsorption of Cr(VI) and As(V) from aqueous solutions: Role of crosslinking metal cations in pH control. *Chem. Eng. J.* **2017**, *307*, 220–229. [[CrossRef](#)]
37. Wang, F.; Guo, C.; Yang, L.R.; Liu, C.Z. Magnetic mesoporous silica nanoparticles: Fabrication and their laccase immobilization performance. *Bioresource Technol.* **2010**, *101*, 8931–8935. [[CrossRef](#)] [[PubMed](#)]
38. Diao, Y.; Wang, Q.; Fu, S. Laccase stabilization by covalent binding immobilization on activated polyvinyl alcohol carrier. *Lett. Appl. Microbiol.* **2002**, *35*, 451–456.
39. Song, X.; Wu, H.; Shi, J.; Wang, X.; Zhang, W.; Ai, Q.; Jiang, Z. Facile fabrication of organic–inorganic composite beads by gelatin induced biomimetic mineralization for yeast alcohol dehydrogenase encapsulation. *J. Mol. Catal. B Enzym.* **2014**, *100*, 49–58. [[CrossRef](#)]
40. Zhang, Y.; Wu, H.; Li, L.; Li, J.; Jiang, Z.; Jiang, Y.; Chen, Y. Enzymatic conversion of Baicalin into Baicalein by  $\beta$ -glucuronidase encapsulated in biomimetic core-shell structured hybrid capsules. *J. Mol. Catal. B Enzym.* **2009**, *57*, 130–135. [[CrossRef](#)]
41. Homaei, A.; Etemadipour, R. Improving the activity and stability of actinidin by immobilization on gold nanorods. *Int. J. Biol. Macromol.* **2015**, *72*, 1176–1181. [[CrossRef](#)] [[PubMed](#)]
42. Antony, N.; Balachandran, S.; Mohanan, P.V. Immobilization of diastase  $\alpha$ -amylase on nano zinc oxide. *Food Chem.* **2016**, *211*, 624–630. [[CrossRef](#)] [[PubMed](#)]
43. Wu, L.; Wu, S.; Xu, Z.; Qiu, Y.; Li, S.; Xu, H. Modified nanoporous titanium dioxide as a novel carrier for enzyme immobilization. *Biosens. Bioelectron.* **2016**, *80*, 59–66. [[CrossRef](#)] [[PubMed](#)]
44. Bradford, M.M. A rapid and sensitive method for the quantitation of microgram quantities of protein utilizing the principle of protein-dye binding. *Anal. Biochem.* **1976**, *72*, 248–254. [[CrossRef](#)]

45. Xia, T.T.; Liu, C.Z.; Hu, J.H.; Guo, C. Improved performance of immobilized laccase on amine-functioned magnetic Fe<sub>3</sub>O<sub>4</sub> nanoparticles modified with polyethylenimine. *Chem. Eng. J.* **2016**, *295*, 201–206. [[CrossRef](#)]
46. Hermanova, S.; Zarevucka, M.; Bousa, D.; Pumera, M.; Sofer, Z. Graphene oxide immobilized enzymes show high thermal and solvent stability. *Nanoscale* **2015**, *7*, 5852–5858. [[CrossRef](#)] [[PubMed](#)]

**Sample Availability:** Not available.



© 2017 by the authors; licensee MDPI, Basel, Switzerland. This article is an open access article distributed under the terms and conditions of the Creative Commons Attribution (CC BY) license (<http://creativecommons.org/licenses/by/4.0/>).